On holographic phase transitions at finite chemical potential

Shunji Matsuura

Perimeter Institute for Theoretical Physics,
Waterloo, Ontario N2L 2Y5, Canada, and
Department of Physics, University of Tokyo,
7-3-1 Hongo, Bunkyoku, Tokyo, 113-0033, Japan
E-mail: smatsuura@perimeterinstitute.ca

ABSTRACT: Recent Holographic studies have shown that N=4 super Yang-Mills theory coupled to fundamental matter with finite chemical potential undergoes a first order phase transition. In this paper, we study N_f D6 probe branes with or without electric field on it in the black D4 brane background compactified on a circle with supersymmetry breaking boundary condition. At energy scales much lower than the compactification scale, the dual gauge theory is effectively four dimensional non-supersymmetric $SU(N_c)$ Yang-Mills theory coupled to fundamental matter with or without baryon number charge. Within the supergravity approximation, the decoupling of the Kaluza-Klein modes is not fully realized. For chemical potential $\mu_b < N_c M_q$ there is a line of first order phase transitions from stable meson phase to unstable meson phase. On the other hand for $\mu_b > N_c M_q$ there is no phase transition and mesons are unstable. A peculiar and interesting property of this system is that for a certain range of chemical potential $\mu_b < N_c M_q$, a new phase transition appears in the unstable meson phase. This phase transition is characterized by a discontinuous change of unstable meson lifetime.

KEYWORDS: Brane Dynamics in Gauge Theories, D-branes.

Contents

1. Introduction

Thermal phase structure of strongly coupled $SU(N_c)$ super Yang-Mills theory at finite chemical potential and finite temperature may be studied by using holographic duality [3, 4]. The holographic method provides a powerful framework to study a broad class of large N_c, strongly coupled gauge theories with a small number N_f of fields in the fundamental representations [9 – 14]. The gravity dual of these gauge fields appear as N_f probe Dq-branes on the near horizon geometries of N_c black Dp-branes.

Particularly interesting physics appears when the system undergoes a confinement/deconfinement phase transition. Above this phase transition temperature T_{dec}, the gluons and the adjoint matters are deconfined and the dual geometry contains a black hole [5]. Since our main understanding of QCD largely comes from the behaviour of fundamental matter, it is interesting to ask how they behave around the deconfinement phase transition. The thermal properties of fundamental matter in the deconfinement phase can be extracted by studying probe D-branes in this black hole background.

In [11, 12], it was show that at zero baryon density, fundamental matter undergoes a first order phase transition at T_{fun}. In the lower temperature phase, the probe D-brane sits entirely outside the black hole horizon, which is called a Minkowski embedding (see figure 1), and the mass spectrum of meson in this phase is discrete and has a mass gap [11, 12]. In the higher temperature phase, a part of the probe D-brane fall through the black hole horizon, which is called a black hole embedding, and the mass spectrum of meson in this phase is continuous and gapless, characterized by quasinormal modes [12, 15, 16]. We emphasize that this is in the deconfinement phase. That means that after the gluons and the adjoint matters are deconfined, the fundamental matter is still in bound states at temperature $T_{dec} < T < T_{fun}$. The meson bound states in the deconfinement phase are also illustrated in related models [18]. On the other hand if T_{fun} is smaller than
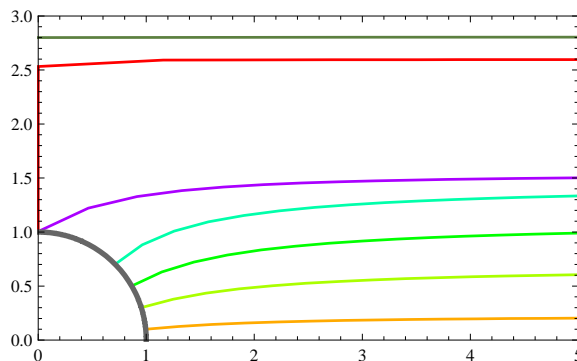
Figure 1: Probe D-brane configurations in the presence of the black hole. Gray circle represents the black hole horizon. For the black hole embeddings, temperature decreases from the bottom to top. The dark green colour represents Minkowski embedding which is entirely outside the horizon. At lower temperature, the probe D-brane is entirely outside the black hole horizon, i.e., the Minkowski embedding.(dark green line). At higher temperature, the probe D-brane partially fall through the black hole horizon, i.e., the black hole embedding.

T_{dec}, the confinement/deconfinement phase transition and the meson melting take place simultaneously. This phenomenon, the stable meson bound states in a deconfinement phase $T_{\text{dec}} < T < T_{\text{fun}}$, is also found in lattice QCD [20], which suggests that bound states of heavy quarks survive after the deconfinement phase transition up to a few T_{fun}.

Motivated by these agreements with QCD, other region of the QCD phase diagram, i.e., finite temperature with finite baryon density n_b or finite chemical potential $\mu_q = \mu_b/N_c$ was investigated in [2, 21 – 26], see also [19]. The introduction of a finite baryon density corresponds to the presence of a U(1) gauge field, which is a diagonal part of the gauge group U(N_f), on the probe D-brane.

In [2], this direction is explicitly investigated in the D3/D7 system. The boundary gauge theory is SU(N_c) $\mathcal{N}$=4 super Yang-Mills theory with N_f $\mathcal{N}$=2 hypermultiplets in the fundamental representation. There, physical quantities such as quark condensate in finite n_b continuously change from those in $n_b = 0$. One of the most crucial difference between zero and nonzero baryon density systems is in the presence finite baryon density, Minkowski embeddings are unphysical and do not play any role, while black hole embeddings cover the whole range of the temperature above deconfinement phase transition. This is different from $n_b = 0$ case where black hole embeddings cover only high temperature region and Minkowski embeddings cover only low temperature region [11, 12]. In the overlapping region, there is a phase transitions from a Minkowski embedding to a black hole embedding.

The reason why Minkowski embeddings are unphysical in the presence of finite baryon density is as follows; The electric field on the D-brane represents dissolved fundamental strings. Since Wess-Zumino coupling is inactive in this brane configuration, fundamental strings never 'leak' from the brane and the local baryon number density is still nonzero above the horizon. Since the fundamental strings cannot terminate, we have to have fundamental strings stretching from the probe D-brane to the horizon. At this junction point,

the tension of the probe D-brane is always smaller than that of the fundamental strings. That means that there is no force balanced configurations in the Minkowski embeddings at finite baryon density and the brane must fall down through the horizon. See [2, 1] for more detail discussions. Instead at very low temperature a black hole embedding mimics a Minkowski embedding, i.e., a very long and narrow spike, which corresponds to a bundle of dissolved fundamental strings on the probe D-brane, stretches down to the horizon. For smaller n_b, there is a first order phase transition from a black hole to another black hole embedding, which is very similar to a Minkowski to a black hole embedding in the zero baryon density case. Above the critical density n_b^*, there is no phase transition anymore.

However it was shown in [2] that there is an unstable region near the phase transition line. It is expected that this unstable region finally decays to other stable state. However since this region minimizes the free energy, there is no state to decay and the final state was missing.

This puzzle was recently addressed in [1]. In the grand canonical ensemble, we fix not a baryon density but a chemical potential. Since a Minkowski embedding can have a finite chemical potential without a baryon density, this embedding is physical in the grand canonical ensemble and plays an important role. The black hole embeddings cover only larger chemical potential or higher temperature region. On the other hand, the Minkowski embeddings cover the whole value of μ with temperature lower than T_{fun} (see figure2 in [1]). There are phase transitions inside the overlapping region from Minkowski to black hole embeddings. One of the most remarkable results is that the unstable region is thermodynamically unfavourable in the grand canonical ensemble. Since in the thermodynamical limit, the grand canonical and the canonical ensemble should give the same answer [28], the unstable region is not a true ground state but it should be replaced by an inhomogeneous phase of a stable black hole embedding and a Minkowski embedding in the canonical ensemble.

The aim of this paper is to investigate the generality of the phase structure in Dp/Dq system. We analyze the D4/D6 system. Physical properties such as the phase transitions from a black hole to a black hole embedding in the canonical ensemble and from a Minkowski to a black hole embedding in the grand canonical ensemble and the existence of the unstable region are the same. However the inhomogeneous phase has a more complicated and interesting structure. There is a new additional phase transition. Figure 2 shows the phase diagram of the D4/D6 system. As in the case of the D3/D7 system, the black hole embeddings cover only high temperature or high chemical potential region. The boundary of the black hole embeddings is plotted in the green line. In the region surrounded by the blue line, there are more than one value of n_q for each μ_q/M_q and $T/\bar{M}$. The red line is the line of the phase transitions. On the scale of (a), the difference between the red and the green line is very subtle. An interesting structure is found in (b) and (c). Near $\mu_q/M_q = 0.16$, $T/\bar{M} = 0.77$, the red line separates into two branches. The upper branch represents phase transitions from black hole to black hole embeddings. In the field theory side, this corresponds to a discontinuous change of meson lifetime. Below this phase transition temperature, the spectral function of mesons would show sharp peaks representing longer lifetime quasiparticles, while above the phase transition, the peaks would be
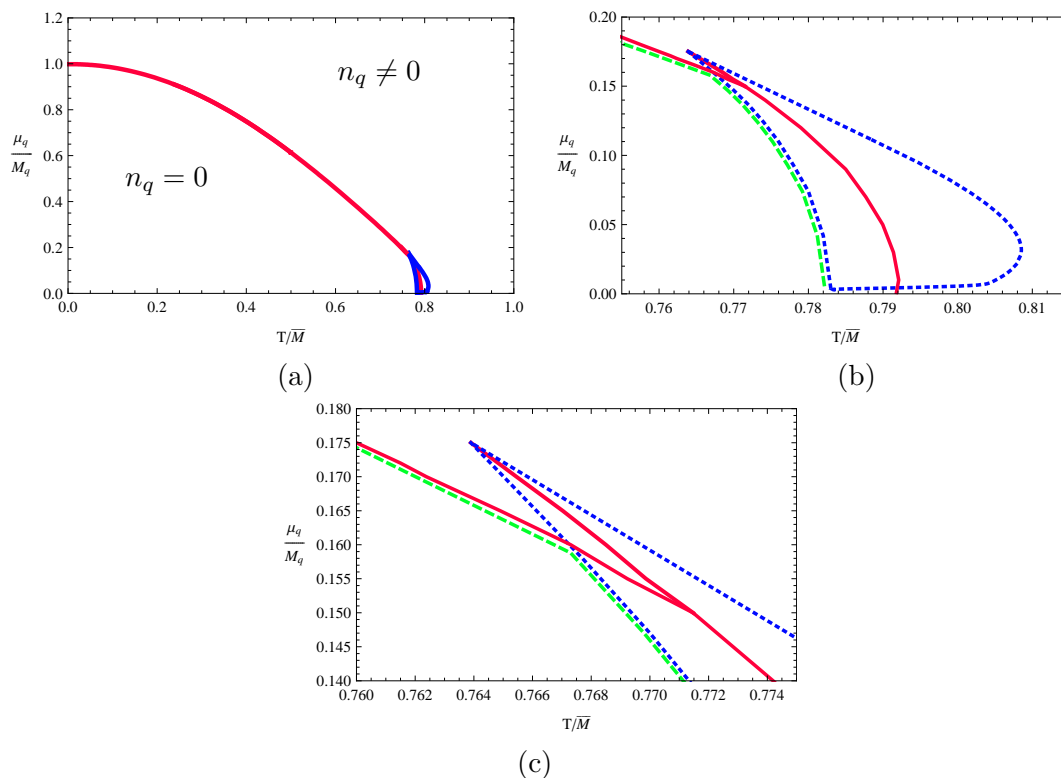
Figure 2: Phase diagram: Quark chemical potential μ_q/M_q versus temperature $T/\bar{M}$. The red line separates the phase of Minkowski embeddings (small temperatures, small μ_q/M_q) from black hole embeddings. Figure (b) zooms in on the region near the end of this line and also depicts the boundary of the region accessed by the black hole embeddings (dashed green) and a small region (enclosed by the dotted blue curve) where more than one black hole embedding in available for a given value of μ_q and T. Figure (c) zooms in on the region near the branches of the red lines. The two branches of the red lines show the phase transitions, the lower one is from the Minkowski embeddings to the black hole embeddings and the upper one is from the black hole embeddings to the black hole embeddings.

flatter and the lifetime of the quasiparticles would be shorter. The lower branch represents phase transitions from Minkowski to black hole embeddings. We will discuss the relation between these phases and the unstable region in section 3.

2. Holographic framework

In this section we explain the D4/D6 system. Closed string modes on the near horizon geometry of D4 brane is dual to maximally supersymmetric five dimensional super Yang-Mills theory with large N_c and at strong coupling on the boundary . In order to obtain four dimensional gauge theory at low energy scale, we compactify one space direction, say x_4, with a radius M_{KK}^{-1}. For energy scale $E \ll M_{\mathrm{KK}}$, the boundary gauge theory is effectively four dimensional. Since we want to study the thermal properties of fundamental fields coupling to Yang-Mills field, we choose the supersymmetry-breaking spin structure,

i.e., the anti-periodic boundary condition for fermions in x_4 direction. The fermions in the vector multiplet get masses of order M_{KK} at tree level and the scalars possibly get masses of order $g_4^2 N_c M_{KK}$ at one loop level. So the gauge theory is effectively non-supersymmetric four dimensional Yang-Mills theory at low energy scale.[1] By fixing the boundary geometry, this system undergoes a phase transition from a thermal AdS phase to an AdS black hole phase at certain temperature T_{dec}. In the dual language, this transition is deconfinement/confinement phase transition [5]. This system describes only adjoint matters. To approach QCD in this holographic framework, quarks or fundamental matter must be included. The introduction of fundamental matter in the holographic framework is demonstrated in [8]. According to their work, a probe D-brane plays a role of fundamental matter in the dual picture. In our case, inserting N_f D6 branes into this black-D4 background corresponds to the coupling of N_f hypermultiplets in the fundamental representation to the Yang-Mills fields with the gauge group $SU(N_c)$. The quarks arise from the lightest mode of the fundamental strings connecting between D4 and D6 branes. In the decoupling limit, the mesons are dual to the fundamental strings whose both ends are attaching on D6 branes. This means that the fluctuations on the D6 branes describe the mesons in the dual gauge theory.

2.1 Black D4 background

The supergravity solution corresponding to the decoupling limit of N_c coincident D4-branes in the black hole phase is in the string frame

$$ds^2 = \frac{1}{2}\left(\frac{\varrho}{L}\right)^{3/2}\left[-\frac{f^2}{\tilde{f}}dt^2 + \tilde{f}dx_4^2\right] + \left(\frac{L}{\varrho}\right)^{3/2}\frac{\tilde{f}^{1/3}}{2^{1/3}}\left[d\varrho^2 + \varrho^2 d\Omega_4^2\right] \tag{2.1}$$

$$e^\Phi = \left(\frac{u}{L}\right)^{3/4} = \left(\frac{\varrho^3}{4L^3}\right)^{1/4}\tilde{f}^{1/2} \tag{2.2}$$

where $f = 1 - \frac{u_0^3}{\varrho^3}$ and $\tilde{f} = 1 + \frac{u_0^3}{\varrho^3}$.[2] u_0 is the location of the horizon and the AdS radius L is given by

$$L^3 = g_s N_c \pi l_s^3. \tag{2.3}$$

Hawking radiation appears in this background with the temperature given by the surface gravity $T = \kappa/2\pi$, or by the regularity of the Euclidean section,

$$T = \frac{3}{4\pi}\sqrt{\frac{u_0}{L^3}}. \tag{2.4}$$

This temperature is identified with the temperature of the boundary gauge theory. The dual boundary gauge theory is maximally supersymmetric Yang-Mills theory on $R^{1,4}$ with coordinates $\{t, \vec{x}_4\}$.

As we explained above, we compactify on a circle with radius $1/M_{KK}$ with supersymmetry breaking boundary condition. At low energy $E \ll M_{KK}$ the effective field theory is

---

[1] However the Kaluza-Klein modes do not decouple within the supergravity approximation [5]. For example, the lightest glueball spectrum is of the same order as the strong coupling scale [7].

[2] This metric (isotropic coordinate) is related to the ordinary coordinate as $(u_0\rho)^{3/2} - u^{3/2} = \sqrt{u^3 - u_0^3}$

four dimensional non-supersymmetric Yang-Mills theory. The string coupling constant in the bulk theory and the gauge coupling constant in the dual boundary theory is related through

$$g_5^2 = (2\pi)^2 g_s l_s, \quad g_4^2 = g_5^2 M_{\text{KK}} \tag{2.5}$$

where $g_s = e^{\phi_\infty}$ and $g_{4,5}$ are the Yang-Mills coupling constants in four and five dimensions.

2.2 D6-brane embeddings

We introduce N_f D6-branes in this background in the following configuration;

	0	1	2	3	4	5	6	7	8	9
D4	×	×	×	×	×					
D6	×	×	×	×			×	×	×	

We split the AdS radial direction and S^4 into two parts so that SO(3)×SO(2) symmetry is manifest. We define the radial coordinate r in (x^5, x^6, x^7) directions and R in (x^8, x^9) directions where $\rho = \varrho/u_0$ is a dimensionless coordinate.

$$\rho^2 = r^2 + R^2, \quad r = \rho \sin\theta, \quad R = \rho \cos\theta, \tag{2.6}$$

and

$$d\rho^2 + \rho^2 d\Omega_4^2 = d\rho^2 + \rho^2(d\theta^2 + \sin^2\theta d\Omega_2^2 + \cos^2\theta d\phi^2) \tag{2.7}$$
$$= dr^2 + r^2 d\Omega_2^2 + dR^2 + R^2 d\phi^2 \tag{2.8}$$

The probe D6 brane embedding is parametrized by a function, $\chi(\varrho) \equiv \cos\theta(\varrho)$. The induced D6 metric is

$$ds^2 = \frac{1}{2}\left(\frac{\varrho}{L}\right)^{3/2}\left[-\frac{f^2}{\tilde{f}}dt^2 + \tilde{f}dx_3^2\right] + \left(\frac{L}{\varrho}\right)^{3/2}\frac{\tilde{f}^{1/3}}{2^{1/3}}\left[\left(1 + \frac{\varrho^2\dot{\chi}^2}{1-\chi^2}\right)d\varrho^2 + \varrho^2\left(1-\chi^2\right)d\Omega_2^2\right] \tag{2.9}$$

Now we introduce U(1) gauge field $A(\varrho)dt$ on the probe D6 branes. The D6 brane action per unit spacetime volume of the gauge theory is

$$I_{D6} = -N_f T_6 \int e^{-\Phi}\sqrt{-\det(P[G]_{ab} + 2\pi\alpha' F_{ab})} \tag{2.10}$$

$$= -N_f T_6 \frac{\Omega_2}{4} \int d\varrho \, \tilde{f}^{4/3}\varrho^2\left(1-\chi^2\right)\sqrt{f^2\tilde{f}^{-2/3}\left(1 + \frac{\varrho^2\dot{\chi}^2}{1-\chi^2}\right) - k\dot{A}^2} \tag{2.11}$$

where

$$k = (2^{2/3}2\pi l_s^2)^2, \tag{2.12}$$

and the D6 brane tension is

$$T_6 = \frac{2\pi}{g_s(2\pi l_s)^7}. \tag{2.13}$$

– 6 –

Let us analyze the behaviour of the electric field A. The electric displacement d is defined by

$$d = \frac{N_f T_6 \Omega_2}{4} \frac{\tilde{f}^{4/3} \varrho^2 (1 - \chi^2) k \dot{A}}{\sqrt{f^2 \tilde{f}^{-2/3}(1 + \frac{\varrho^2 \dot{\chi}^2}{1 - \chi^2}) - k \dot{A}^2}} \tag{2.14}$$

The electric displacement represents the number density of dissolved fundamental strings in the D6 branes. With the similar analysis to [2, 1] the electric displacement identified with the string number density n_q: $d = n_q$. Since the action does not explicitly depend on A, the equation of motion for A is $d =$ constant, or

$$\dot{A} = \frac{d f \tilde{f}^{-\frac{1}{3}} \sqrt{1 + \frac{\varrho^2 \dot{\chi}^2}{1 - \chi^2}}}{\sqrt{d^2 k + \left(\frac{N_f T_6 \Omega_2 k}{4}\right)^2 \tilde{f}^{8/3} \varrho^4 (1 - \chi^2)^2}} \tag{2.15}$$

$$\tag{2.16}$$

Asymptotically χ goes to zero and f and $\tilde{f}$ go to one. The leading order of the equation is then

$$\dot{A} = \frac{d}{\frac{N_f T_6 \Omega_2 k}{4} \varrho^2} + \mathcal{O}\left(\frac{1}{\rho^3}\right) \tag{2.17}$$

So the asymptotic behaviour of the gauge field is

$$A \sim \mu_q - \frac{4d}{N_f T_6 \Omega_2 k} \frac{1}{\varrho} + \cdots \tag{2.18}$$

where μ is

$$\mu_q = d \int_{u_0}^{\infty} d\varrho \frac{f \tilde{f}^{-\frac{1}{3}} \sqrt{1 + \frac{\varrho^2 \dot{\chi}^2}{1 - \chi^2}}}{\sqrt{d^2 k + \left(\frac{N_f T_6 \Omega_2 k}{4}\right)^2 \tilde{f}^{8/3} \varrho^4 (1 - \chi^2)^2}}. \tag{2.19}$$

Here we set $A(u_0) = 0$. This condition comes from the regularity of the one form at the horizon. The horizon contains a bifurcation surface where a Killing vector ∂_t vanishes. In order for the gauge field, which is a one form $A_t dt$, to be well defined, the component A_t must vanish there. See also [2, 12].

According to the holographic dictionary, the dual operator is schematically

$$\mathcal{O}_q = \psi^\dagger \psi + q^\dagger \mathcal{D}_t q \tag{2.20}$$

where ψ and q are left and right Weyl fermions and scalar fields (see also [2]). From (2.18) and (2.20), we identify μ_q with a quark chemical potential.

For convenience, we also use dimensionless quantities and a gauge field,

$$\tilde{d} = \frac{4}{N_f T_6 \Omega_2 \sqrt{k}} \frac{d}{u_0^2}, \quad \tilde{\mu} = \frac{\sqrt{k}}{u_0} \mu, \quad \tilde{A} = \frac{\sqrt{k}}{u_0} A. \tag{2.21}$$

The equation of motion for χ is

$$\frac{d}{d\varrho}\left(f\tilde{f}\frac{\varrho^4\dot{\chi}}{\sqrt{1+\frac{\varrho^2\dot{\chi}^2}{1-\chi^2}-\frac{k\dot{A}^2}{f^2\tilde{f}^{-2/3}}}}\right)$$
$$+\left(f\tilde{f}\frac{\varrho^2\chi}{\sqrt{1+\frac{\varrho^2\dot{\chi}^2}{1-\chi^2}-\frac{k\dot{A}^2}{f^2\tilde{f}^{-2/3}}}}\right)\left(2+\frac{\varrho^2\dot{\chi}^2}{1-\chi^2}-2\frac{k\dot{A}^2}{f^2\tilde{f}^{-2/3}}\right)=0 \quad (2.22)$$

The boundary conditions for $\chi(\rho)$ at the horizon is determined by the regularity and it gives $\chi\big|_{\rho=1}=\chi_0$ and $d\chi/d\rho\big|_{\rho=1}=0$ for $0\le\chi<1$. For Minkowski embeddings it is convenient to use R,r coordinates instead of χ,ρ coordinates. The boundary conditions for Minkowski embeddings at $r=0$ are $R\big|_{r=0}=R_0$ and $dR/dr\big|_{r=0}=0$ for $1<R_0$. The asymptotic forms ($\rho\to\infty$) for χ is

$$\chi\sim\frac{m}{\varrho}+\frac{c}{\varrho^2}+\mathcal{O}\left(\frac{1}{\varrho^3}\right) \quad (2.23)$$
$$=\frac{\tilde{m}}{\rho}+\frac{\tilde{c}}{\rho^2}+\mathcal{O}\left(\frac{1}{\rho^3}\right), \quad (2.24)$$

where we define dimensionless quantities

$$\tilde{m}=\frac{m}{u_0}=\frac{3^2 m}{(4\pi)^2 L^3 T^2}, \quad \tilde{c}=\frac{c}{u_0^2}=\frac{3^4 c}{(4\pi)^4 L^6 T^4}. \quad (2.25)$$

Holography relates these quantities to a quark mass and a condensate [10] by

$$M_q=\frac{u_0\tilde{m}}{2^{\frac{5}{3}}\pi l_s^2} \quad (2.26)$$
$$<\mathcal{O}_m>=-2^{5/3}\pi^2 l_s^2 N_f T_{D6} u_0^2\tilde{c} \quad (2.27)$$

A bare quark mass M_q is an asymptotic distance between D4 and D6 brane in flat space. The operator $\mathcal{O}_m$ is the variation of the mass term in the microscopic Lagrangian, i.e., $\mathcal{O}_m=-\partial_{M_q}\mathcal{L}$, and the schematic form is

$$\mathcal{O}_m=\bar{\psi}\psi+q^\dagger\Phi q+M_q q^\dagger q, \quad (2.28)$$

where Φ is one of the adjoint scalars. See also [2, 12]. We assume that the vacuum expectation value of the fundamental scalar fields q vanishes because whenever the scalar fields acquire the nonzero expectation value, the energy density increases [10]. In that case, $<\mathcal{O}_m>$ is equal to $<\bar{\psi}\psi>$ and represents a quark condensation. Given the above result, we show various figures in terms of $T/\bar{M}\equiv1/\sqrt{\tilde{m}}$.

Let us study more on the chemical potential. Once the equation of motion for $\chi(\varrho)$ (2.22) is solved, the chemical potential is obtained from (2.19). In general, we have to resort to numerical calculation. However, we can extract analytic properties in the limiting cases of small and high temperatures. First we consider low temperature or large bare
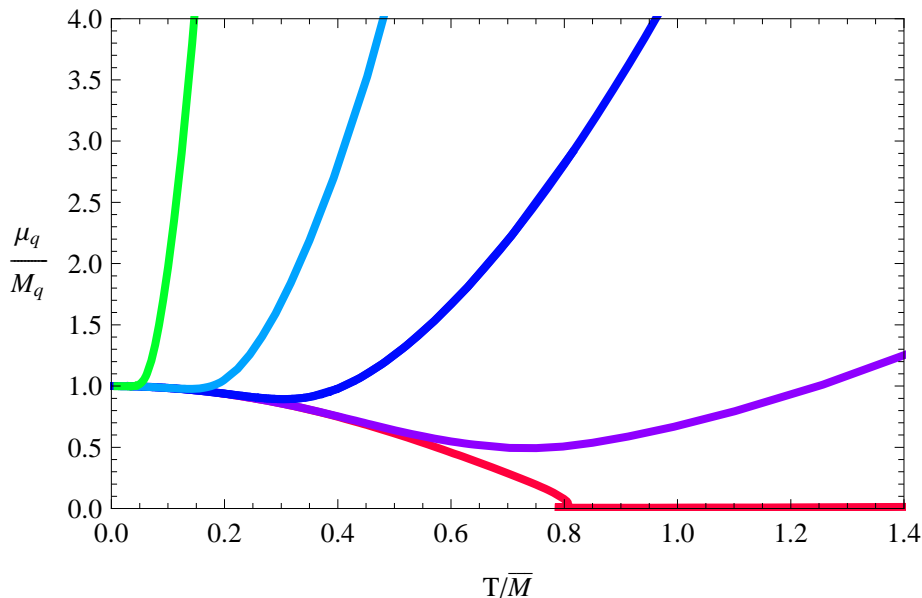
Figure 3: Chemical potential μ_q/M_q versus $T/\bar{M}$ for various values of $\tilde{d}$, increasing from bottom up: $\tilde{d} = 10^{-2}, 1, 10, 100, 10^4$.

quark mass limit $T/\bar{M} \to 0$. As shown in figure 1, at very low temperature the probe D-brane goes up straight from the horizon u_0 to $\sim m$. The main contribution to the distance between the D4 and D6 brane, or $T/\bar{M}$, comes from this part. Under this approximation,

$$\mu_q = d \int_{u_0}^{\infty} d\varrho \frac{f \tilde{f}^{-\frac{1}{3}} \sqrt{1 + \frac{\varrho^2 \dot{\chi}^2}{1-\chi^2}}}{\sqrt{d^2 k + \left(\frac{N_f T_6 \Omega_2 k}{4} \right)^2 \tilde{f}^{8/3} \varrho^4 (1-\chi^2)^2}} \tag{2.29}$$

$$\simeq d \int_{u_0}^{m} d\varrho \frac{f \tilde{f}^{-\frac{1}{3}}}{\sqrt{d^2 k}} \tag{2.30}$$

$$\simeq m/\sqrt{k} = M_q \tag{2.31}$$

Regardless of d, μ_q goes to M_q. This is consistent with figure 3 where all curves with different $\tilde{d}$ meet on the vertical axis at $\mu_q/M_q = 1$. On the opposite limit, i.e., high temperature or small bare quark mass limit $T/\bar{M} \to \infty$, the probe D6 branes are almost flat and intersect the horizon at the equator. Plugging $\chi \simeq 0$ and $u_0 \gg 1$ into the equation, the leading contribution is

$$\mu_q \simeq \frac{4d}{(N_f T_6 \Omega_2 k)} \frac{1}{2^{2/3} u_0} + \mathcal{O}(d^3) \tag{2.32}$$

$$= \frac{9}{4 N_f N_c} \frac{n_q}{T^2} + \mathcal{O}(n_q^3) \tag{2.33}$$

There are some notable points. The first point is that for any value of n_b, μ_q goes to zero as temperature goes to infinity. In this sense, figure 3 might be misleading. Each line in the figure shows μ_q/M_q versus $T/\bar{M}$ for fixed $\tilde{d}$ not d. In each line, higher temperature

corresponds to a higher baryon number density and lower temperature corresponds to a lower baryon number density. The second point is for fixed μ_q, n_b changes as $\sim T^2$. Since in the grand canonical ensemble we survey fix μ_q planes, this equation suggests that the baryon density monotonically increases at very high temperature for any fixed μ_q/M_q.

3. Thermodynamics

We move on to the thermodynamics of the D6 brane, or the fundamental matter. As we will see the canonical ensemble is not a suitable one for studying the phase diagram since it includes an unstable region. Our main focus here is the grand canonical ensemble. A similar unstable region can also be found in the D3/D7 system [1]. We will briefly mention on the canonical ensemble.

Euclidean path integral of D6 branes give thermal partition function [27]. Since the classical solution of the equation of motion is the saddle point of the path integral, the on-shell action gives main contribution to the Gibbs free energy W, i.e., $W = TI_E$. From the grand canonical point of view, a brane configuration which minimizes the Gibbs free energy is thermodynamically favourable. However, naive calculation of thermal quantities include divergences from IR region. For example, we can clearly see that the action diverges as

$$\int d\rho\rho^2 \simeq \frac{\rho_{\max}^3}{3}. \tag{3.1}$$

In order to obtain physically meaningful, finite quantities, we need to renormalize them. The renormalization procedure of probe D-brane is studied in [29]. According to that, renormalization is done by introducing boundary terms for probe branes on the cut-off plane so that the divergences cancel. For the D4/D6 case, this boundary term is concretely studied in [12]. Before starting the detail analysis, we define a normalization constant

$$\mathcal{N} = \frac{\pi}{T}N_f T_{D6}u_0^3. \tag{3.2}$$

Inserting the asymptotic expansion of χ and $\dot{A}$ int (2.11), the action is

$$\frac{I_{\text{reg}}}{\mathcal{N}} = \int d\rho\rho^2 \left(1 - \frac{\tilde{m}^2}{\rho^2} - \frac{2\tilde{m}\tilde{c}}{\rho^2}\right)\left(1 + \frac{\tilde{m}^2}{2\rho^2}\cdots - \frac{\tilde{d}^2}{2\rho^4}\right). \tag{3.3}$$

The contribution to the action from the gauge field is the term proportional to $\tilde{d}^2$. This gives no new divergence. So we can use the same boundary term as that of $\tilde{d}=0$ case to renormalize the divergence. We apply the following boundary term per unit spacetime volume of the gauge field [12],

$$I_{\text{bound}} = -\frac{\Omega_2}{3}L^3 T_6 N_f\sqrt{\gamma}\left(1 - \frac{3}{2}\chi^2\right)|_{\rho=\rho_{\max}} \tag{3.4}$$

$$= -\frac{u_0^3\Omega_2 T_6 N_f}{12}\left(\rho_{\max}^3 - \frac{3}{2}\tilde{m}^2\rho_{\max} - 3\tilde{m}\tilde{c}\right), \tag{3.5}$$

where γ is the induced metric at $\rho = \rho_{\max}$

$$ds_\gamma^2 = \frac{1}{2}\left(\frac{u_0\rho_{\max}}{L}\right)^{3/2}\left(-\frac{f(\rho_{\max})^2}{\tilde{f}(\rho_{\max})}dt^2 + \tilde{f}(\rho_{\max})\,dx_3^2\right). \tag{3.6}$$

The total action is then,

$$\frac{I_{\mathrm{tot}}}{\mathcal{N}} = \frac{I_{\mathrm{reg}}}{\mathcal{N}} + \frac{I_{\mathrm{bound}}}{\mathcal{N}} \tag{3.7}$$

$$= \left[G(\tilde{m},\dot{\tilde{A}}) - \frac{1}{3}\left(\rho_{\min}^3 - \frac{3}{2}\tilde{m}^2\rho_{\min} - 3\tilde{m}\tilde{c}\right)\right], \tag{3.8}$$

where $G(\tilde{m},\dot{\tilde{A}})$ is

$$G(\tilde{m},\dot{\tilde{A}}) = \int_{\rho_{\min}}^{\infty} d\rho\left(\tilde{f}^{4/3}\rho^2\left(1-\chi^2\right)\sqrt{f^2\tilde{f}^{-2/3}\left(1+\frac{\rho^2\dot{\chi}^2}{1-\chi^2}\right) - \dot{\tilde{A}}^2} - \rho^2 + \frac{\tilde{m}^2}{2}\right) \tag{3.9}$$

From the thermodynamical point of view, this action is identified the Gibbs free energy $W(T,\mu_q)$ via $W = TI_E$.

In the canonical ensemble with fixed n_q, we use the Helmholtz free energy. Similar to [2, 30], the Helmholtz free energy is associated with the Legendre transform of I_E.

$$\frac{\tilde{I}_E}{\mathcal{N}} = \frac{I_{D6}}{\mathcal{N}} + \frac{\int d\dot{A}}{\mathcal{N}} \tag{3.10}$$

which is function of the temperature and the baryon density. We identify $F(T,n_q) = TI_E$ where $F(T,n_q)$ is the Helmholtz free energy. Since there is no contribution from the electric displacement to the boundary term , the Legendre transformed action is

$$\frac{\tilde{I}_E}{\mathcal{N}} = H(\tilde{m},\tilde{d}) - \frac{1}{3}\left(\rho_{\min}^3 - \frac{3}{2}\tilde{m}^2\rho_{\min} - 3\tilde{m}\tilde{c}\right) \tag{3.11}$$

where $H(\tilde{m},\tilde{d})$ is

$$H(\tilde{m},\tilde{d}) = \int_{\rho_{\min}}^{\infty} d\rho\left[f\tilde{f}^{-1/3}\sqrt{1+\frac{\rho^2\dot{\chi}^2}{1-\chi^2}}\sqrt{\tilde{f}^{8/3}\rho^4(1-\chi^2)^2 + \tilde{d}^2} - \rho^2 + \frac{\tilde{m}^2}{2}\right]. \tag{3.12}$$

We evaluated the free energy numerically. The qualitative feature is very similar to that of the D3/D7 system (see figure 9 and 10 in [2]). For smaller value of $\tilde{d}/\tilde{m}^2$, there is a line of first order phase transition from black hole to black hole embeddings and above a critical value $\left(\tilde{d}/\tilde{m}^2\right)^*$ there is no phase transition. Note that since $\tilde{d}$ depends on a temperature n_q/T^4, we use a temperature independent quantity $\tilde{d}/\tilde{m}^2 \sim n_q/M_q^2$ as a parameter. The blue line in figure 9 shows the phase transition line in the canonical ensemble. The critical temperature and baryon density is $T/\bar{M} = 0.7786$ and $\tilde{d}/\tilde{m}^2 = 0.041$.
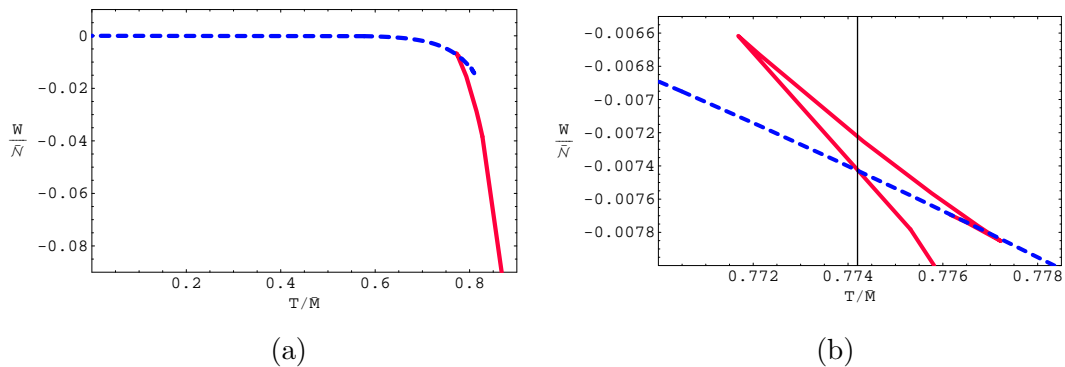
Figure 4: Free energy versus temperature for $\mu_q/M_q = 0.14$. The blue dotted (red solid) line represents the Minkowski (black hole) branch. The vertical line marks the temperature of the phase transition.
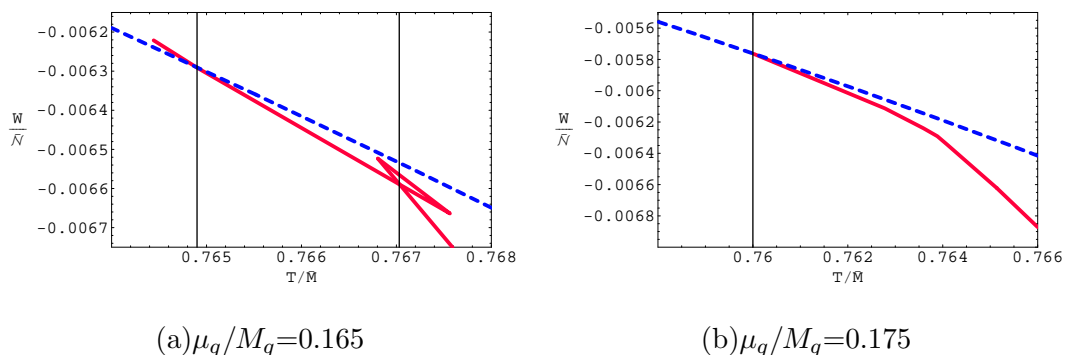

(a)μ_q/M_q=0.165   (b)μ_q/M_q=0.175

Figure 5: Free energy versus temperature for (a)μ_q/M_q=0.165 and (b)μ_q/M_q=0.175. (a) shows that there are two phase transitions. One is from the Minkowski embedding to the black hole embedding at $T/\bar{M} = 0.765$ and the other is from the black hole embedding to the black hole embedding at $T/\bar{M} = 0.767$. (b) shows that there is only one phase transition from the Minkowski embedding to the black hole embedding at $T/\bar{M} = 0.76$. The vertical lines mark the temperature of the phase transitions.

3.1 Phase transitions in the grand canonical ensemble

As we mentioned in section 1, the black hole embeddings cover only above the green line in figure 2 while the Minkowski embeddings cover whole value of μ_q/M_q below $\sim T_{\text{fun}}$. This suggests that there is a line of first order phase transitions for $\mu_q/M_q < 1$ in the grand canonical ensemble. Thermodynamically favourable embeddings minimize the Gibbs free energy for give temperature and chemical potential. In this section, we calculate the free energy for various μ_q/M_q.

Figure 4(a) shows the Gibbs free energy W normalized by $\bar{\mathcal{N}}$ versus temperature $T/\bar{M}$ for $\mu_q = 0.14$ in a broad view and figure 4(b) shows a zoomed in around the phase transition. Here the normalization is $\bar{\mathcal{N}} = \mathcal{N}\bar{M}$. The red line is the black hole embedding and the dashed blue line is the Minkowski embedding. The starting point of the red line $(T/\bar{M} = 0.776, W/\bar{\mathcal{N}} = -0.0077)$ is $\tilde{d} = 10^{-3}$. As $\tilde{d}$ becomes larger, the temperature becomes higher and the free energy becomes smaller, then at $\tilde{d} = 5 \times 10^{-2}$ the temperature
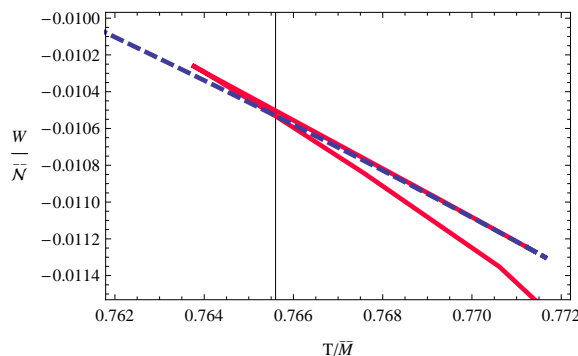
Figure 6: Free energy versus temperature for $\mu_q/M_q = 0.005$ in the D3/D7 system. There is only one turnover in the black hole embeddings. This should be compared with the D4/D6 system (figure 4) where there are two turnovers.

starts to decrease and the free energy starts increase. And at $\tilde{d} = 0.17$, the temperature turns to increase and the free energy turns decrease again. As μ increases, the starting point of the free energy of the black hole embedding at very small $\tilde{d}$ goes in the left above direction and the three fold structure starts to form a swallow tail shape. At a critical value of μ_q/M_q=0.15, the crossing point of the swallow tail goes down below the line of the Minkowski free energy. Above this critical value, there are two phase transitions. The first one is from a Minkowski embedding to a black hole embedding. The second one is from a black hole embedding to another black hole embedding. A representative of this phase is shown in figure 5(a). At $\mu_q/M_q = 0.165$, there is phase transition from a Minkowski embedding to a black hole embedding at $T/\bar{M} = 0.765$ and there is a phase transition from a black hole embedding to a black hole embedding at $T/\bar{M} = 0.767$. As μ becomes larger, the swallow tail shrinks smaller and smaller and finally at $\mu_q/M_q = 0.175$ the black hole to black hole phase transition disappears. The free energy at this value of μ_q/M_q is shown in figure 5(b). There is a phase transition at $T/\bar{M} = 0.76$ and this is the only phase transition in this phase. These three fold structures in the D4/D6 system should be compared to the figure 6 which shows the typical phase transition for $\mu_q < M_q$ in the D3/D7 system (see also figure 4 in [1]). The only phase transition is from a Minkowski embedding to a black hole embedding and there is no phase transition from a black hole to a black hole embedding.

This feature can also be seen from other perspective. Figure 7(a) shows $\tilde{d}/\tilde{m}^2$ versus $T/\bar{M}$ diagram near the phase transition for $\mu_q/M_q = 0.16$. As explained above, below a certain temperature there are only Minkowski embeddings. Around $T/\bar{M} = 0.7668$ black hole embeddings appear. However the Minkowski embeddings are still favoured. At $T/\bar{M} = 0.7673$, the free energy of the black hole embedding becomes equal to the Minkowski embedding and the system jumps from $\tilde{d}/\tilde{m}^2 = 0$ to $\tilde{d}/\tilde{m}^2 = 0.0034$ (A) As temperature increases, the system goes along the red line until it meets another phase transition point(B). At $T/\bar{M} = 0.7685$, $\tilde{d}/\tilde{m}^2 = 0.0146$ (B), the system jumps to a configuration which has the same chemical potential but larger value of $\tilde{d}/\tilde{m}^2 = 0.0708$(D) in a
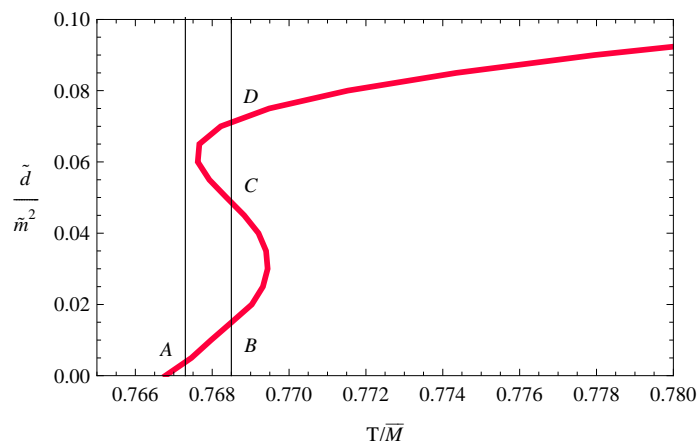
(a) Baryon density versus temperature in D4/D6
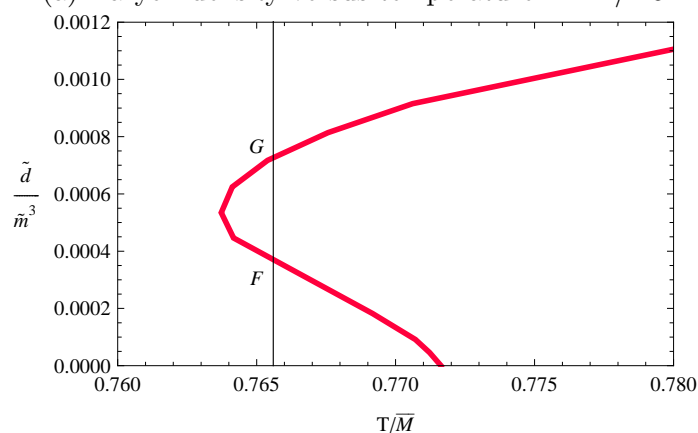
(b) The same in D3/D7

Figure 7: Baryon density versus temperature for (a) $\mu_q/M_q = 0.16$ in the D4/D6 system and (b) $\mu_q/M_q = 0.005$ in the D3/D7 system. In the D4/D6 system, baryon density is a triple-valued function of temperature while in the D3/D7 system, baryon density is a double-valued function of temperature.

black hole embedding. Above this temperature, there is no phase transition and as $T/\bar{M}$ becomes larger $\tilde{d}/\tilde{m}^2$ becomes larger.

We also show a $\tilde{d}/\tilde{m}^3$ versus $T/\bar{M}$ diagram for $\mu_q/M_q = 0.005$ in the D3/D7 system in figure 7(b). As above, below a certain temperature there are only Minkowski embeddings. At $T/\bar{M} = 0.7656$, the free energy of the Minkowski embedding and the black hole embedding coincides and the first order phase transition occurs from $\tilde{d}/\tilde{m}^3 = 0$ to $\tilde{d}/\tilde{m}^3 = 0.00073(G)$. Clearly $\mu_q/\bar{M}_q$ is a two-valued function of $T/\bar{M}$ while it is a triple-valued function in the case of the D4/D6 system, and the region corresponding to (A)-(B) in figure 7(a) is missing.

In the rest of this section, we address another interesting property, i.e., the instability in the canonical ensemble, and combine it with the phase transitions discussed above. The
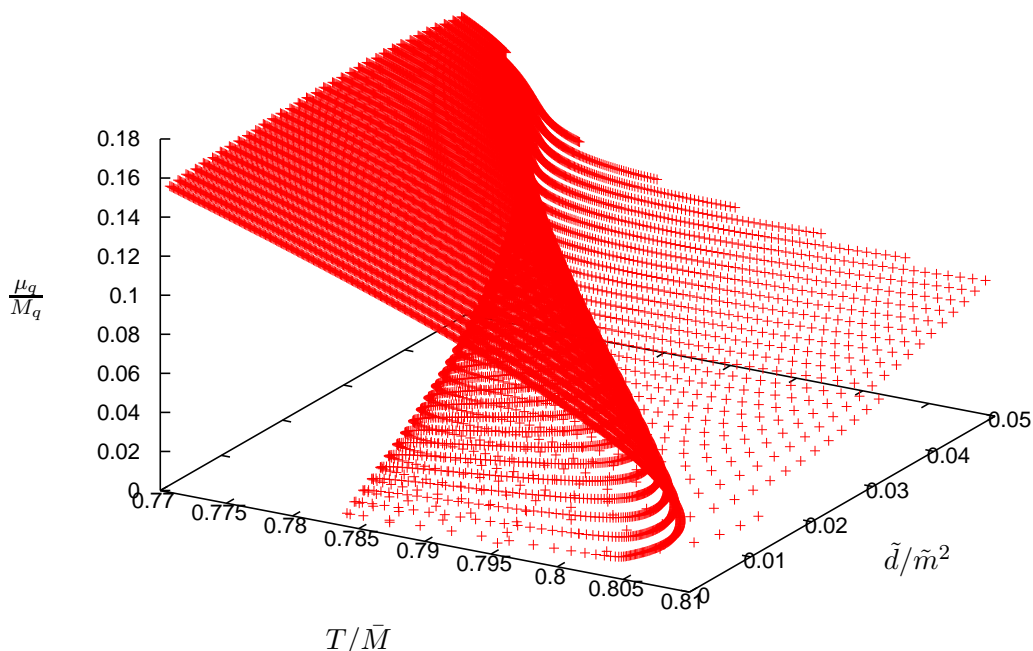
Figure 8: Three-dimensional plot of the chemical potential, the temperature and the charge density determined by black hole embeddings.

conditions for the stability of the system are given

$$\left.\frac{\partial S}{\partial T}\right|_{\mu_q} > 0, \quad \left.\frac{\partial n_b}{\partial \mu_q}\right|_T > 0. \tag{3.13}$$

The unstable configuration can be found by examining μ_q/M_q versus $T/\bar{M}$ and $\tilde{d}/\tilde{m}^2$ diagram(figure 8). This figure covers only a small range of the surface near the phase transition in the canonical ensemble. For fixed n_b, or $\tilde{d}/\tilde{m}^2$, the system jumps from the top to the bottom of the surface at certain temperature. Thermodynamical point of view, this means that only the region of the top of this fold with temperature lower the phase transition and of the bottom of this fold with temperature higher than the phase transition is favoured. Other region are thermodynamically unfavoured do not come into the stability discussion. An interesting point is that on the top of the fold and just below the phase transition temperature we can actually find a region where thermodynamically favourable but electrically unstable. This region should play a central role in the canonical ensemble. In [1], the similar problem was addressed. The resolution of the problem in the D3/D7 system was that minimizing the free energy in the grand canonical ensemble always picks out either a stable black hole embedding or Minkowski embedding. Hence the system never
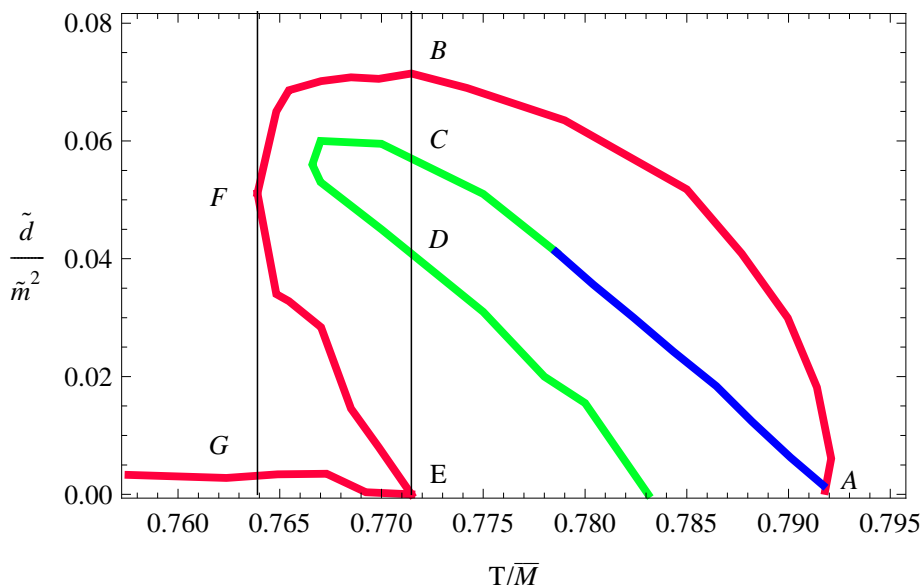
Figure 9: Baryon density at the phase transition in the grand canonical ensemble (red) The blue line of phase transitions identified in the canonical ensemble at fixed n_b. The region enclosed by the green and blue curves corresponds to the unstable region in which $(\partial \mu_q / \partial n_q)_T < 0$.

suffer from the instability. The question is whether the same is true for the D4/D6 system. After explaining figure 9, we come back to this question.

Figure 9 shows the black hole to Minkowski phase transition, $\partial \mu_q / \partial n_b = 0$, and the canonical phase transition line. The blue line is the canonical phase transition line. For fixed value of d, there is a black hole to black hole phase transition at this line. The green line is a part of the $\frac{\partial \mu_q}{\partial n_b}\big|_T = 0$ line. The region surrounded by green and blue line is the thermodynamically favourable but electromagnetically unstable region. The red line is the mapping of the phase transition line in figure 2 to $\tilde{d}/\tilde{m}^2 - T/\bar{M}$ plane. Let us explain this line more detail. In figure 4(b), there is one phase transition from the black hole embedding to the Minkowski embedding at $T = 0.7742$ and $\tilde{d}/\tilde{m}^2 = 0.069$. This corresponds to the red line between A and B in figure 9. In this region there is only one value of $\tilde{d}/\tilde{m}^2$ for fixed $T/\bar{M}$ and at this point the phase transition occurs from a Minkowski embedding to a black hole embedding, i.e., from a point at $\tilde{d}/\tilde{m}^2 = 0$ to a point on the red line with the same temperature.

In figure 5(a), there are two phase transitions. One is from the Minkowski embedding to the black hole embedding at $T/\bar{M} = 0.7649$ and $\tilde{d}/\tilde{m}^2 = 0.0034$. The other one is from the black hole embedding at $T/\bar{M} = 0.76703$ and $\tilde{d}/\tilde{m}^2 = 0.0285$ to the other black hole embedding at $T/\bar{M} = 0.76703$ and $\tilde{d}/\tilde{m}^2 = 0.07014$ This configuration corresponds to a region between the two vertical black lines in figure 9. The first phase transition is from a Minkowski embedding $\tilde{d}/\tilde{m}^2 = 0$ to a point on the red line between E and G. Then the second phase transition occurs at a different temperature from a point on the red line between E and F to a point on the red line between F and B.

In figure 5(b), there is only one phase transition from the Minkowski embedding to

the black hole embedding at $T/\bar{M} = 0.76$ and $\tilde{d}/\tilde{m}^2 = 0.003$. This corresponds to the left part of G on the red line.

As in the D3/D7 system [1], the whole unstable region is surrounded by the red line. Hence the grand canonical ensemble picks out either stable black hole embedding or Minkowski embedding; the thermodynamically favourable phases discussed above are all stable. The unstable region appeared in the canonical ensemble is misidentified the ground state since we restricted our analysis to the homogeneous configurations. The true ground state is an inhomogeneous phase of stable phases [1].

The true ground state of the region surrounded by the red curve A-B and the $\tilde{d}/\tilde{m}^2 = 0$ axis is an inhomogeneous phase of stable black hole (on the red curve A-B) embedding and Minkowski embedding (on the $\tilde{d}/\tilde{m}^2 = 0$ axis). The true ground state of the region surrounded by B-F-E-B is an inhomogeneous phase of stable black hole embedding (on the red curve B-F) and another stable black hole embedding (on the red curve F-E). The true ground state of the region surrounded by the red curve E-G and the $\tilde{d}/\tilde{m}^2 = 0$ axis, is an inhomogeneous phase of stable black hole embedding (on the red curve E-F) and a Minkowski phase (on the $\tilde{d}/\tilde{m}^2 = 0$ axis). Hence both in the grand canonical ensemble and the canonical ensemble, the unstable region is thermodynamically unfavourable.

4. Conclusion and discussion

We have seen that there are several common physical properties in the Dp/Dq systems with finite charge density and chemical potential. In the grand canonical ensemble there is a line of the first order phase transitions from Minkowski to black hole embeddings found in [24–26, 1]. The black hole embeddings cover high $T/\bar{M}$ or high μ_q/M_q region while the Minkowski embeddings cover the whole μ_q/M_q region with $T/\bar{M}$ smaller than $\sim T_{\text{fun}}$. In the supersymmetric limit $T/\bar{M} \to 0$, μ_q/M_q always goes to one for any value of n_b, i.e., the energy which is necessary to add one quark in the system is equal to its bare mass. In this limit black hole embeddings exactly look like Minkowski embeddings. There is a very thin and long spike stretching from Dq branes down to Dp branes. In the dual field theory point of view [12, 15, 16], the Minkowski embeddings correspond to the stable meson phase and he spectral function consists of a series of delta-function-like peaks, i.e., resonances centred on mass eigenvalues. On the other hand, the black hole embeddings correspond to the unstable meson phase and the spectral function is continuous. In the canonical ensemble, there is a line of first order phase transitions from black hole to black hole embeddings for charge density less than n_b^* and above this critical density there is no phase transition. Just below the phase transition temperature, there is an electrodynamically unstable region. However this unstable region is not the true ground state and should be replaced by an inhomogeneous phase.

We also have seen that there is a difference between the D3/D7 and D4/D6 system. In the D3/D7 system for fixed $\mu_q < M_q$, there is only one phase transition, from a Minkowski to a black hole embedding. On the other hand, in the D4/D6 system for certain range of $\mu_q < M_q$, there are two phase transitions, one is from a Minkowski to a black hole embedding and the other one is from a black hole to another black hole embedding. Following

the investigation of [15, 17, 23], we can give a physical interpretation of this black hole to black hole embedding phase transition in the dual gauge theory. The feature of the spectral function is characterized by the poles of the corresponding retarded correlators in the complex frequency plane. In the Minkowski embeddings, the poles are on the real axis and the spectral function is, as mentioned above, a series of delta-function-like peaks. In the black hole embeddings, the poles are located apart from the real axis. At lower temperature, the imaginary part of the poles are close to the real axis and the spectral function exhibits distinct peaks. As temperature increases, the poles move away from the real axis and the spectral function becomes featureless. Hence our black hole to black hole phase transition from lower temperature to higher temperature would correspond to poles jumping from closer locations to the real axis to farther locations. The peaks of the spectral function would become lower and the lifetime of the quasiparticles would become shorter. It would be very interesting to investigate this point concretely. Lattice QCD studies [20] suggest that meson bound states survive the deconfinement phase transition and the bound states dissolve at T_{fun}. As explained, Minkowski to black hole phase transition represents this meson dissolving phase transition. A very interesting question is then what the phase transition in QCD corresponding to the black hole to black hole phase transition is. It would be an exotic phase transition if it exists in QCD.

Before ending the section, we comment one more common property in the D3/D7 and the D4/D6 systems. As mentioned above, in the $T/\bar{M} \to 0$ limit, the chemical potential μ_q goes to M_q. This result is reasonable in the case of free fermions with zero density. However since our system is strongly interacting system with bosons and fermions, the reason is not very clear. In fact, the chemical potential is very close to the constituent mass at the phase transition points not only at $T/\bar{M} = 0$ but also for a broad range of temperature except the canonical phase transition region. Hence the quarks behave as if they were 'free' particles. We have put 'free' om quotes because the constituent mass takes into account all the corrections from the quarks and the adjoint plasma. The constituent quark mass is defined by the energy of a fundamental string stretching from a probe D-brane to the horizon in a Minkowski embedding. This constituent quark mass at $T/\bar{M} = 0$ on Minkowski embeddings with $n_q = 0$ was calculated in [12, 31, 1] The induced metric of the fundamental string stretching from a probe D-brane to the horizon in R direction is

$$ds^2 = \frac{1}{2} \left(\frac{u_0 R}{L} \right)^{3/2} \left[-\frac{f^2}{\tilde{f}} dt^2 \right] + \left(\frac{L}{u_0 R} \right)^{3/2} \frac{\tilde{f}^{1/3}}{2^{1/3}} u_0^2 dR^2. \tag{4.1}$$

The Nambu-Goto action for the fundamental string is

$$I = -\frac{1}{2\pi l_s^2} \int_1^{R_0} dR dt \sqrt{-\det P[G]} \tag{4.2}$$

$$= -\frac{1}{2\pi l_s^2} \int dt \frac{u_0}{2^{2/3}} \left(\left(1 + \frac{1}{R_0^3} \right)^{2/3} R_0 - 2^{2/3} \right) \tag{4.3}$$

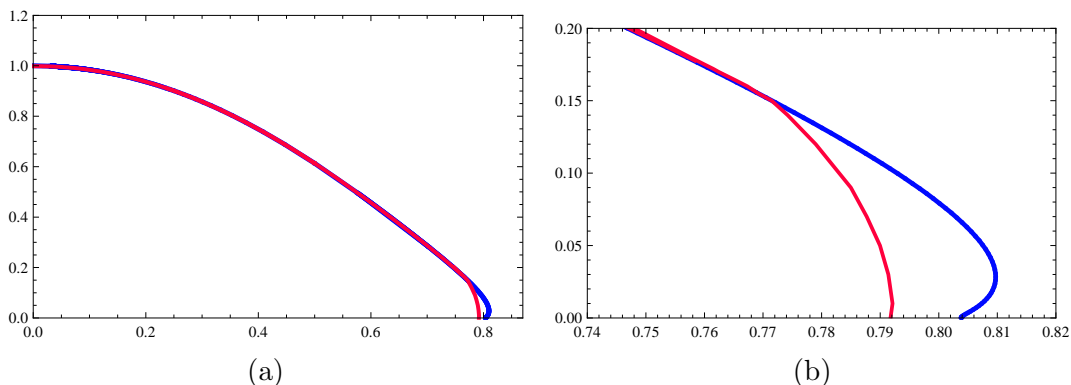Identifying the constituent mass to minus the action per unit time of this static configura-

Figure 10: Comparison of the ratio M_c/M_q (blue) with the ratio μ_q/M_q (red) at which the phase transition from a Minkowski to a black hole embedding takes place. The two curves essentially coincide on the scale of the figure (a).

tion, we have

$$M_c = \frac{1}{2\pi l_s^2} \frac{u_0}{2^{2/3}} \left(\left(1 + \frac{1}{R_0^3} \right)^{2/3} R_0 - 2^{2/3} \right). \tag{4.4}$$

We can see that the constituent mass is almost identical to the chemical potential except near the canonical phase transition region. This result is the same as that of the D3/D7 system [1] and the similar result is obtained in [25]. As mentioned in [1], this result is surprising because the quark density is much larger than the size of an individual quark;

$$n_q = \frac{2^{3/2}}{3^3} N_f N_c g_{\mathrm{eff}}(M_q) \left(\frac{\tilde{d}}{\tilde{m}^2} \right) n_{\mathrm{crit}}, \tag{4.5}$$

where $g_{\mathrm{eff}}^2(M_q) = \lambda M_q = g_5^2 N_c M_q$ and $n_{\mathrm{crit}} = \bar{M}^3$. Structure functions [32] or a quark's disturbance of the adjoint fields [33] in the D3/D7 system are well studied. The mass spectrum of mesons in the Dp/Dq system is discussed in [35]. Motivated by their works, we assume that the individual quark size is $\sim m_{\mathrm{gap}}$. Combining it with the relation $\bar{M}/m_{\mathrm{gap}} \simeq 0.233$ [12], we define the critical density as $n_{\mathrm{crit}} = \bar{M}^3$ at which quarks start to overlap each other. For the effective coupling, supergravity approximation is valid only in the region [34]

$$1 \ll g_{\mathrm{eff}} \ll N_c^{4/3}. \tag{4.6}$$

Hence although $\left(\tilde{d}/\tilde{m}^2 \right)$ may be of order 10^{-3}, n_q is much larger than n_{crit} and interactions would not be negligible.

Acknowledgments

References

[1] D. Mateos, S. Matsuura, R.C. Myers and R.M. Thomson, *Holographic phase transitions at finite chemical potential*, *JHEP* **11** (2007) 085 [arXiv:0709.1225].

[2] S. Kobayashi, D. Mateos, S. Matsuura, R.C. Myers and R.M. Thomson, *Holographic phase transitions at finite baryon density*, *JHEP* **02** (2007) 016 [hep-th/0611099].

[3] J.M. Maldacena, *The large-N limit of superconformal field theories and supergravity*, *Adv. Theor. Math. Phys.* **2** (1998) 231 [*Int. J. Theor. Phys.* **38** (1999) 1113] [hep-th/9711200].

[4] O. Aharony, S.S. Gubser, J.M. Maldacena, H. Ooguri and Y. Oz, *Large-N field theories, string theory and gravity*, *Phys. Rept.* **323** (2000) 183 [hep-th/9905111].

[5] E. Witten, *Anti-de Sitter space, thermal phase transition and confinement in gauge theories*, *Adv. Theor. Math. Phys.* **2** (1998) 505 [hep-th/9803131].

[6] E. Witten, *Baryons and branes in Anti de Sitter space*, *JHEP* **07** (1998) 006 [hep-th/9805112].

[7] C. Csaki, H. Oouguri, Y. Oz and J. Terning, *Glueball mass spectrum from supergravity*, *JHEP* **01** (1999) 017 [hep-th/9806021];
R. de Mello Koch, A. Jevicki, M. Mihailescu and J.P. Nunes, *Evaluation of glueball masses from supergravity*, *Phys. Rev.* **D 58** (1998) 105009 [hep-th/9806125];
H. Ooguri, H. Robins and J. Tannenhauser, *Glueballs and their Kaluza-Klein cousins*, *Phys. Lett.* **B 437** (1998) 77 [hep-th/9806171];
J.A. Minahan, *Glueball mass spectra and other issues for supergravity duals of QCD models*, *JHEP* **01** (1999) 020 [hep-th/9811156];
N.R. Constable and R.C. Myers, *Spin-two glueballs, positive energy theorems and the AdS/CFT correspondence*, *JHEP* **10** (1999) 037 [hep-th/9908175];
R.C. Brower, S.D. Mathur and C.-I. Tan, *Glueball spectrum for QCD from AdS supergravity duality*, *Nucl. Phys.* **B 587** (2000) 249 [hep-th/0003115].

[8] A. Karch and L. Randall, *Open and closed string interpretation of SUSY CFT's on branes with boundaries*, *JHEP* **06** (2001) 063 [hep-th/0105132];
A. Karch and E. Katz, *Adding flavor to AdS/CFT*, *JHEP* **06** (2002) 043 [hep-th/0205236].

[9] J. Babington, J. Erdmenger, N.J. Evans, Z. Guralnik and I. Kirsch, *Chiral symmetry breaking and pions in non-supersymmetric gauge/gravity duals*, *Phys. Rev.* **D 69** (2004) 066007 [hep-th/0306018];
I. Kirsch, *Generalizations of the AdS/CFT correspondence*, *Fortschr. Phys.* **52** (2004) 727 [hep-th/0406274].

[10] M. Kruczenski, D. Mateos, R.C. Myers and D.J. Winters, *Towards a holographic dual of large-N_c QCD*, *JHEP* **05** (2004) 041 [hep-th/0311270].

[11] D. Mateos, R.C. Myers and R.M. Thomson, *Holographic phase transitions with fundamental matter*, *Phys. Rev. Lett.* **97** (2006) 091601 [hep-th/0605046].

[12] D. Mateos, R.C. Myers and R.M. Thomson, *Thermodynamics of the brane*, *JHEP* **05** (2007) 067 [hep-th/0701132].

[13] D. Mateos, R.C. Myers and R.M. Thomson, *Holographic viscosity of fundamental matter*, *Phys. Rev. Lett.* **98** (2007) 101601 [hep-th/0610184].

[14] T. Albash, V.G. Filev, C.V. Johnson and A. Kundu, *A topology-changing phase transition and the dynamics of flavour*, hep-th/0605088;
A. Karch and A. O'Bannon, *Chiral transition of N = 4 super Yang-Mills with flavor on a 3-sphere*, *Phys. Rev.* **D 74** (2006) 085033 [hep-th/0605120];
T. Albash, V.G. Filev, C.V. Johnson and A. Kundu, *Global currents, phase transitions and chiral symmetry breaking in large-N_c gauge theory*, hep-th/0605175;
A. Karch and A. O'Bannon, *Metallic AdS/CFT*, *JHEP* **09** (2007) 024 [arXiv:0705.3870];
A. O'Bannon, *Hall conductivity of flavor fields from AdS/CFT*, *Phys. Rev.* **D 76** (2007) 086007 arXiv:0708.1994.

[15] R.C. Myers, A.O. Starinets and R.M. Thomson, *Holographic spectral functions and diffusion constants for fundamental matter*, arXiv:0706.0162.

[16] C. Hoyos, K. Landsteiner and S. Montero, *Holographic meson melting*, *JHEP* **04** (2007) 031 [hep-th/0612169].

[17] D. Mateos and L. Patino, *Bright branes for strongly coupled plasmas*, arXiv:0709.2168.

[18] O. Aharony, J. Sonnenschein and S. Yankielowicz, *A holographic model of deconfinement and chiral symmetry restoration*, *Ann. Phys. (NY)* **322** (2007) 1420 [hep-th/0604161];
A. Parnachev and D.A. Sahakyan, *Chiral phase transition from string theory*, *Phys. Rev. Lett.* **97** (2006) 111601 [hep-th/0604173];
Y.-H. Gao, W.-S. Xu and D.-F. Zeng, *Ngn, QCD_2 and chiral phase transition from string theory*, *JHEP* **08** (2006) 018 [hep-th/0605138];
K. Peeters, J. Sonnenschein and M. Zamaklar, *Holographic melting and related properties of mesons in a quark gluon plasma*, *Phys. Rev.* **D 74** (2006) 106008 [hep-th/0606195];
E. Antonyan, J.A. Harvey and D. Kutasov, *The Gross-Neveu model from string theory*, *Nucl. Phys.* **B 776** (2007) 93 [hep-th/0608149].

[19] J. Erdmenger, R. Meyer and J.P. Shock, *AdS/CFT with flavour in electric and magnetic Kalb-Ramond fields*, arXiv:0709.1551.

[20] T. Umeda, K. Nomura and H. Matsufuru, *Charmonium at finite temperature in quenched lattice QCD*, *Eur. Phys. J.* **C 39S1** (2005) 9 [hep-lat/0211003];
M. Asakawa and T. Hatsuda, *J/psi and eta/c in the deconfined plasma from lattice QCD*, *Phys. Rev. Lett.* **92** (2004) 012001 [hep-lat/0308034];
S. Datta, F. Karsch, P. Petreczky and I. Wetzorke, *Behavior of charmonium systems after deconfinement*, *Phys. Rev.* **D 69** (2004) 094507 [hep-lat/0312037];
A. Jakovac, P. Petreczky, K. Petrov and A. Velytsky, *On charmonia survival above deconfinement*, hep-lat/0603005;
G. Aarts et al., *Charmonium spectral functions in $N_f = 2$ QCD at high temperature*, PoS(LAT2006)126 [hep-lat/0610065];
G. Aarts, C. Allton, J. Foley, S. Hands and S. Kim, *Spectral functions at non-zero momentum in hot QCD*, PoS(LAT2006)134 [hep-lat/0610061];
P. Petreczky, *Lattice QCD at finite temperature*, *Nucl. Phys.* **A 785** (2007) 10 [hep-lat/0609040];
G. Aarts, C. Allton, J. Foley, S. Hands and S. Kim, *Spectral functions at small energies and the electrical conductivity in hot, quenched lattice QCD*, *Phys. Rev. Lett.* **99** (2007) 022002 [hep-lat/0703008];
H.B. Meyer, *A calculation of the shear viscosity in* SU(3) *gluodynamics*, *Phys. Rev.* **D 76** (2007) 101701 [arXiv:0704.1801];

G. Aarts, C. Allton, M.B. Oktay, M. Peardon and J.-I. Skullerud, *Charmonium at high temperature in two-flavor QCD*, `arXiv:0705.2198`.

[21] R. Apreda, J. Erdmenger, N. Evans and Z. Guralnik, *Strong coupling effective Higgs potential and a first order thermal phase transition from AdS/CFT duality*, *Phys. Rev.* **D 71** (2005) 126002 [`hep-th/0504151`].

[22] K.-Y. Kim, S.-J. Sin and I. Zahed, *Dense hadronic matter in holographic QCD*, `hep-th/0608046`;
N. Horigome and Y. Tanii, *Holographic chiral phase transition with chemical potential*, *JHEP* **01** (2007) 072 [`hep-th/0608198`];
A. Parnachev and D.A. Sahakyan, *Photoemission with chemical potential from QCD gravity dual*, *Nucl. Phys.* **B 768** (2007) 177 [`hep-th/0610247`];
S.K. Domokos and J.A. Harvey, *Baryon number-induced Chern-Simons couplings of vector and axial-vector mesons in holographic QCD*, *Phys. Rev. Lett.* **99** (2007) 141602 [`arXiv:0704.1604`];
Y. Kim, C.-H. Lee and H.-U. Yee, *Holographic nuclear matter in AdS/QCD*, `arXiv:0707.2637`;
O. Bergman, G. Lifschytz and M. Lippert, *Holographic nuclear physics*, `arXiv:0708.0326`;
M. Rozali, H.-H. Shieh, M. Van Raamsdonk and J. Wu, *Cold nuclear matter in holographic QCD*, `arXiv:0708.1322`;
K.-Y. Kim, S.-J. Sin and I. Zahed, *The chiral model of Sakai-Sugimoto at finite baryon density*, `arXiv:0708.1469`.

[23] J. Erdmenger, M. Kaminski and F. Rust, *Holographic vector mesons from spectral functions at finite baryon or isospin density*, `arXiv:0710.0334`.

[24] S. Nakamura, Y. Seo, S.-J. Sin and K.P. Yogendran, *A new phase at finite quark density from AdS/CFT*, `hep-th/0611021`; *Baryon-charge chemical potential in AdS/CFT*, `arXiv:0708.2818`.

[25] K. Ghoroku, M. Ishihara and A. Nakamura, *D3/D7 holographic gauge theory and chemical potential*, `arXiv:0708.3706`.

[26] A. Karch and A. O'Bannon, *Holographic thermodynamics at finite baryon density: some exact results*, `arXiv:0709.0570`.

[27] S.W. Hawking, *The path-integral approach to quantum gravity*, in *General relativity: an Einstein centenary survey*, S.W. Hawking and W. Israel eds., Cambridge University Press, U.K. (1979).

[28] See, for example, D. Ruelle, *Statistical mechanics: rigorous results*, Benjamin, New York, U.S.A. (1969).

[29] A. Karch, A. O'Bannon and K. Skenderis, *Holographic renormalization of probe D-branes in AdS/CFT*, *JHEP* **04** (2006) 015 [`hep-th/0512125`].

[30] A. Chamblin, R. Emparan, C.V. Johnson and R.C. Myers, *Holography, thermodynamics and fluctuations of charged AdS black holes*, *Phys. Rev.* **D 60** (1999) 104026 [`hep-th/9904197`]; *Charged AdS black holes and catastrophic holography*, *Phys. Rev.* **D 60** (1999) 064018 [`hep-th/9902170`].

[31] C.P. Herzog, A. Karch, P. Kovtun, C. Kozcaz and L.G. Yaffe, *Energy loss of a heavy quark moving through N = 4 supersymmetric Yang-Mills plasma*, *JHEP* **07** (2006) 013 [`hep-th/0605158`].

[32] S. Hong, S. Yoon and M.J. Strassler, *Quarkonium from the fifth dimension*, *JHEP* **04** (2004) 046 [hep-th/0312071].

[33] J.L. Hovdebo, M. Kruczenski, D. Mateos, R.C. Myers and D.J. Winters, *Holographic mesons: adding flavor to the AdS/CFT duality*, *Int. J. Mod. Phys.* **A 20** (2005) 3428.

[34] N. Itzhaki, J.M. Maldacena, J. Sonnenschein and S. Yankielowicz, *Supergravity and the large-N limit of theories with sixteen supercharges*, *Phys. Rev.* **D 58** (1998) 046004 [hep-th/9802042].

[35] R.C. Myers and R.M. Thomson, *Holographic mesons in various dimensions*, *JHEP* **09** (2006) 066 [hep-th/0605017].